Twenty years of giant exoplanets - Proceedings of the Haute Provence Observatory Colloquium, 5-9 October 2015
Edited by I. Boisse, O. Demangeon, F. Bouchy & L. Arnold

Structure and evolution of transiting giant planets: a Bayesian homogeneous determination of orbital and physical parameters

A. S. Bonomo[1], S. Desidera[2], M. Damasso[1], A. F. Lanza[3], A. Sozzetti[1], S. Benatti[2], F. Borsa[4], S. Crespi[5], and the GAPS team

Talk given at OHP-2015 Colloquium

[1] INAF - Osservatorio Astrofisico di Torino, via Osservatorio 20, 10025 Pino Torinese, Italy (bonomo@oato.inaf.it)
[2] INAF - Osservatorio Astronomico di Padova, Vicolo dell'Osservatorio 5, 35122, Padova, Italy
[3] INAF - Osservatorio Astrofisico di Catania, via S. Sofia 78, 95123, Catania, Italy
[4] INAF - Osservatorio Astronomico di Brera, Via E. Bianchi 46, 23807 Merate (LC), Italy
[5] Dipartimento di Fisica dell'Università degli studi di Milano, via Celoria, 16, 20133 Milano, Italy

Abstract

We present a Bayesian homogeneous determination of orbital and physical parameters of a large sample of 211 giant transiting planets with masses between 0.1 and 24 $M_{\rm Jup}$ and precision on mass estimates better than 30%. We analyse new high-precision radial velocities for forty-five of them obtained with the HARPS-N@TNG spectrograph to improve and, in some cases, to revise the measure of their orbital eccentricity, and to search for long-period companions. From the updated orbital eccentricities we put constraints on the modified tidal quality factors of giant planets and their host stars. Our comprehensive study 1) allows for improved understanding of orbital evolution and migration scenarios for giant planets, and 2) provides the much needed benchmark statistics for thorough investigations of the diversity of giant planet densities and interior structures.

1 Introduction

Despite the more and more raising interest in discovering and characterising small planets, many fascinating issues concerning the properties and orbital evolution of giant planets are still open. Among these are the migration of close-in giant planets, the origin of the frequently observed spin-orbit misalignments, and the architecture of planetary systems with hot Jupiters.

Two main scenarios are usually invoked to explain the migration of hot giant planets: disc-driven and high-eccentricity migration. The former would yield small eccentricities and obliquities (unless the disc was primordially misaligned by a distant stellar companion) because of damping by the disc (e.g., Goldreich & Tremaine 1980, Papaloizou & Larwood 2000). According to the latter scenario, giant planets can get very close to their stars by moving along highly eccentric orbits excited by planet-planet scattering and/or Kozai-type perturbations. These orbits are eventually circularised by tidal dissipation leading to a close-in planet on a circular orbit (e.g., Rasio & Ford 1996, Fabrycky & Tremaine 2007).

Planets that migrated from high-eccentricity orbits through tidal dissipation and underwent orbit circularisation without significant mass or orbital angular momentum loss are expected to be found at a distance greater or equal than twice the Roche limit $a_{\rm R} = 2.16 \cdot R_{\rm p} \cdot (M_\star/M_{\rm p})^{1/3}$ from their host star (e.g., Faber et al. 2005).

To yield more and more observable constraints to theoretical models of giant planet migration and star-planet tidal interactions, it is important to i) determine accurate orbital and physical parameters with realistic uncertainties for a large sample of giant planets, hopefully estimated in a homogeneous way; ii) acquire more RV data to improve the measure of the orbital eccentricity which is a key parameter to understand planetary evolution (e.g., Damiani & Lanza 2015); iii) search for outer companions to understand better their influence on the orbital parameters of inner hot and warm giant planets; and iv) study the properties of giant planets (eccentricity, alignment, semi-major axis,

etc.) in single and multiple systems (e.g., Knutson et al. 2014). Our work aims precisely at performing a homogeneous analysis of orbital and physical parameters of a large sample of the known transiting giant planets (hereafter, TGP), by including also new radial velocities for 45 systems obtained with the high-resolution and high-precision HARPS-N spectrograph at the Telescopio Nazionale Galileo (Cosentino et al. 2012). This homogeneous analysis is really worthwhile for several reasons:

- planet eccentricities are often fixed to zero in the discovery papers when found consistent with zero and/or different from zero but with a low significance. Even though in some cases this assumption may be justified, it prevents us from determining the uncertainty on the eccentricity and, when this is large, small but significant eccentricities in principle cannot be excluded;

- radial-velocity (RV) data of some planetary systems discovered by independent groups and obtained by these groups with different spectrographs, were never combined to improve the orbital solution;

- RV jitter terms were not often included as free parameters in the orbital fit. This may lead to an underestimation of the uncertainty of the eccentricity and, in the worst cases, even to spurious eccentricities (Husnoo et al. 2012, hereafter H12);

- previous homogeneous analyses by Pont et al. (2011) (hereafter P11) and H12 were limited to less than seventy systems while more than two hundred TGP are known today.

2 Giant sample and radial-velocity data

We selected 211 TGP that satisfy the following criteria: i) have masses $0.1 < M_{\rm p} < 24$ $M_{\rm Jup}$ and uncertainty on the mass lower than 30%, ii) do not belong to compact multi-planet systems, hence either they are alone or have cold companions, and iii) were published before 2014 (we have recently added those published in 2015 for a forthcoming paper).

For each system, we analysed all the RV datasets published in the literature with at least four RV observations at different orbital phases. Additionally, for 45 systems we acquired new RV measurements with the HARPS-N spectrograph at TNG within the GAPS (Global Architecture of Planetary System) collaboration. In particular, at least six HARPS-N RVs spread over $\sim$ 2.5 yr, with a typical precision of a few m/s, were obtained for each of the 45 targets.

3 Data analysis

Literature and our new HARPS-N data were fitted with i) a Keplerian orbit model; ii) a Keplerian orbit and a long-term drift, when residuals obtained with the simple Keplerian orbit show a significant ($\geq 3\sigma$) slope caused by either an outer planetary/stellar companion or a stellar activity cycle ; iii) two Keplerians with a possible long-term drift, if the inner TGP has a known long-period companion; iv) a Keplerian orbit and a curvature if data cover less than half of the period of the outer companion or the stellar activity cycle. RV zero points and jitter terms for each dataset were fitted along with the orbital parameters.

Gaussian priors were imposed on the conjunction time and orbital period from transit photometry as well as on the times of secondary eclipses, when available, observed from space and/or from the ground. Uniform priors were considered for the orbital eccentricity and the RV semi-amplitude, and Jeffrey's priors were used for the jitter terms.

The posterior distributions of the orbital parameters were obtained in a Bayesian framework by using a differential evolution Markov chain Monte Carlo (DE-MCMC) code, which is the MCMC version of the DE genetic algorithm (Ter Braak 2006). It guarantees an optimal exploration of the parameter space and fast convergence through the automatic choice of step scales and orientations to sample the posterior distributions (Eastman et al. 2013; Bonomo et al. 2015). Convergence and well mixing of the DE-MCMC chains were achieved following Ford (2006).

The newly determined orbital parameters for each system were then combined with the literature values of stellar mass, orbital inclination, and planetary radius to derive updated values of planetary masses and densities.

4 Results

4.1 Eccentricities

We found two new significant eccentricities that were not reported in the literature. On the contrary, four previously reported eccentric orbits are consistent with zero, according to our analysis. In some cases, especially when there are no secondary eclipse observations, our new HARPS-N RV measurements allowed us to improve the precision of the orbital eccentricity by a factor ranging between 3 and 10. Figure 1 shows our HARPS-N RV data of WASP-13 (the blue circles) along with the literature (SOPHIE) measurements (green circles). We found $e < 0.017$ to be compared with the measure $e = 0.14 \pm 0.10$ obtained by considering only the literature values (Skillen et al. 2009).

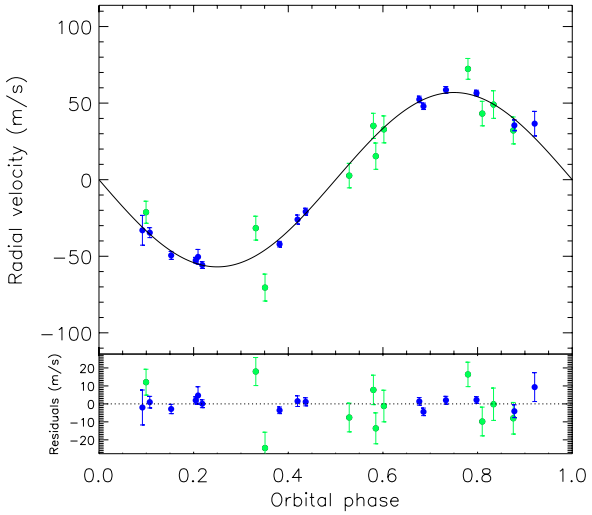

Figure 1: HARPS-N (blue circles) and SOPHIE (green circles) RV measurements of WASP-13. Note the high-accuracy and precision radial velocities collected with HARPS-N with respect to the literature data.

4.2 Long-term trends and outer companions

Limiting ourselves to the 45 systems we monitored with HARPS-N, we found that two of them show linear trends with the same slope as reported in the literature while three others have different or inverted slopes (curvature). Among these latter is XO-2N even though, unlike Knutson et al. (2014), we attribute its curvature to an activity cycle instead of an outer companion because our RV residuals, after subtracting the orbit of the hot Jupiter XO-2b, are strongly correlated with the Ca II activity indicator $\log R'_{\rm HK}$ (Damasso et al. 2015a). We didn't find any linear trend in two systems with previously reported slope but this could be still consistent with the presence of outer companions if our HARPS-N data sampled the maximum/minimum of the curvature.

We discovered the long-period companion KELT-6c ($P = 1267 \pm 80$ d, $a = 2.39 \pm 0.11$ au, $M_{\rm p} \sin i = 3.7 \pm 0.2\ M_{\rm Jup}$, $e = 0.21 \pm 0.04$) of the hot Jupiter KELT-6b ($P = 7.84$ d, $a = 0.084 \pm 0.001$ au, $M_{\rm p} \sin i = 0.44 \pm 0.02\ M_{\rm Jup}$, $e < 0.04$) of which we measured a slight misalignment through the observation of the Rossiter-McLaughling effect $\lambda = -36 \pm 11$ deg (Damasso et al. 2015b). This system thus joins the handful of hot Jupiters with a cold companion and a measured projected obliquity, that is HAT-P-13b, HAT-P-17b, WASP-8b, WASP-41b, and WASP-47b. All of them are aligned with the exception of WASP-8 which is also eccentric. The other eccentric planet of this sample, HAT-P-17b, is on the contrary aligned. Clearly, a much greater sample of close-in giant planets with outer planetary companions and both eccentricity and obliquity accurate measurements is certainly required to infer the influence of wide-orbit companions on the inner planet orbital parameters.

4.3 The curious case of TrES-4b

Our HARPS-N data of TrES-4b revealed an unexpected surprise: we found that the RV semi-amplitude $K = 51 \pm 3$ m/s is approximately half of that derived by Mandushev et al. (2007), that is $K = 97 \pm 7$ m/s. The reason of this disagreement is not fully understood yet but the high-accuracy and high-precision HARPS-N data leave no doubts about the reliability of our new K measure. The latter implies a much lower planetary mass $M_\mathrm{p} \sin i = 0.49 \pm 0.03\ M_\mathrm{Jup}$ than reported in the literature, hence a lower density of 0.099 ± 0.015 g/cm^3 (Sozzetti et al. 2015), that makes TrES-4b the hot Jupiter with the second lowest density known, WASP-17b being the record-holder at present.

4.4 Updated tidal diagram of giant transiting planets

Figure 2 shows the updated tidal diagram first suggested by P11 where mass ratios $M_\mathrm{p}/M_\star$ are plotted vs a/R_p because the circularisation time τ_e scales as $\tau_e \propto (M_\mathrm{p}/M_\star)^2 \cdot (a/R_\mathrm{p})^5$ (e.g., Hut 1981). In this diagram empty circles show the position of giant planets with well-determined circular orbits, that is with eccentricities consistent with zero and 1σ uncertainties $\sigma_e < 0.05$; crosses indicate planets with orbits that are likely circular but have large uncertainties on the orbital eccentricity $\sigma_e > 0.05$; orange triangles are related to significant but small eccentricities, i.e. $e \leq 0.1$; and blue squares indicate eccentricities higher than 0.1. Moreover, the solid and dashed lines show the position of a planet with $R_\mathrm{p} = 1.2\ R_\mathrm{Jup}$ and semi-major axis $a = a_\mathrm{R}$ and $a = 2a_\mathrm{R}$. The dotted line displays the 1-Gyr circularisation time scale for $P = 3$ d, $Q'_\mathrm{p} = 10^6$, and $e = 0$, where $Q'_\mathrm{p} = 3Q_\mathrm{p}/2k_2$ is the planetary modified tidal quality factor, Q_p is the planet tidal quality factor, and k_2 is the Love number (e.g., Murray & Dermott 1999). Q'_p is a parameterisation of the response of the planet's interior to tidal perturbation: the higher Q'_p, the lower the dissipation rate of the kinetic energy of the tides inside the planet. A similar definition applies to the stellar modified quality factor Q'_s.

As first noticed by P11 and H12, this diagram shows that the giant planet orbital parameters are shaped by star-planet tidal interactions. Indeed, all the transiting giant planets with $e > 0.1$ (blue squares) have large separations and/or relatively high mass ratios. Moreover, most of them are found on the right side of the 1-Gyr circularisation time scale. With this updated tidal diagram, we are able to confirm some previously identified trends but now with a sample that is approximately three times bigger than earlier analyses: a) planets with $M_\mathrm{p}/M_\star \lesssim 10^{-3}$ stop at the circularisation radius $a \geq 2a_\mathrm{R}$; b) a handful of those with $10^{-2} \lesssim M_\mathrm{p}/M_\star \lesssim 10^{-3}$ are found closer to their host star ($a_\mathrm{R} < a < 2a_\mathrm{R}$); c) there is a dearth of close-in circular planets with $M_\mathrm{p}/M_\star \gtrsim 4 \cdot 10^{-3}$. These massive planets likely rise tides in the star strong enough for angular momentum exchange and tidal decay so they end up being engulfed by their host star. However, this scarcity might be partially explained also with the higher inertia of massive planets to gravitational scattering towards inner orbits by lighter planetary companions and/or a less efficient formation in discs that are not massive enough.

4.5 The α distribution

The $\alpha = a/a_\mathrm{R}$ distribution is shown in Fig. 3 for both well-determined circular orbits (solid line) and likely circular orbits (dashed line) but with relatively large uncertainties ($\sigma_e > 0.05$). In the vast majority of cases $a > 2a_\mathrm{R}$, with a peak at $\alpha \sim 2.75$ although the shape of this distribution is also affected by the transit probability implying that the discovery of closer-in planets is more likely than outer ones. Therefore, the peak may not be the most likely value of the underlying planet distribution. Nonetheless, if $\alpha > 2$ is a clear signature of tidal dissipation from high-eccentric orbits as outlined by Faber et al. (2005), the high-eccentricity migration would be favoured over the disk migration.

4.6 Variation range for the modified tidal quality factors

After identifying circular and eccentric orbits, we can estimate the upper and lower limits of Q'_p. Following Matsumura et al. (2008), an upper limit on Q'_p simply comes from the constraint that circularisation time must be lower than the system (or stellar) age for clearly circular planets ($\sigma_e < 0.05$). On the contrary, lower limits on both Q'_p and Q'_s can be derived by imposing that the circularisation time must be longer than the system age for eccentric orbits, if we assume that the eccentricity is not presently excited by a third body in the system.

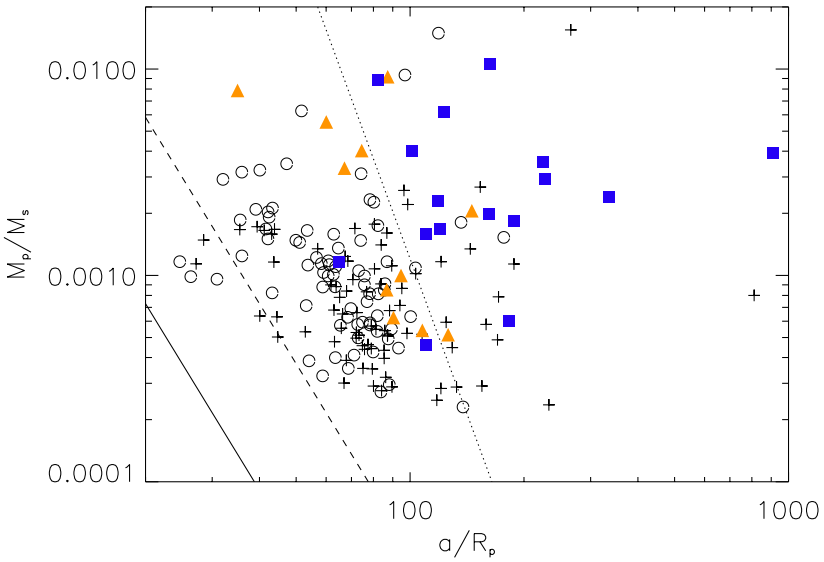

Figure 2: Updated tidal diagram of the 211 transiting giant planets considered in this study. Empty circles show the position of giant planets with well-determined circular orbits, that is with eccentricities consistent with zero and 1σ uncertainty $\sigma_e < 0.05$; crosses indicate likely circular orbits but with large uncertainties $\sigma_e > 0.05$; orange triangles display significant but small eccentricities, i.e. $e \leq 0.1$; and blue squares $e > 0.1$. Solid and dashed lines show the position of a planet with $R_p = 1.2\,R_{Jup}$ and semi-major axis $a = a_R$ and $a = 2a_R$. The dotted line displays the 1-Gyr circularisation time scale for $P = 3$ d, $Q'_p = 10^6$, and $e = 0$.

Figures 4 and 5 show the upper and lower limits of Q'_p as a function of the semi-major axis. Planets at orbital distances greater than 0.04 au have $Q'_p \lesssim 2 \cdot 10^7$, those with smaller semi-major axes might have even higher Q'_p corresponding to very low internal dissipation.

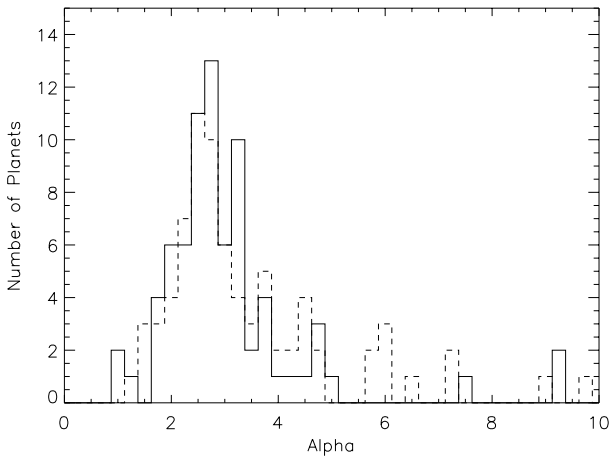

Figure 3: Distribution of $\alpha = a/a_R$ for well-determined circular orbits ($\sigma_e < 0.05$, solid line) and likely circular orbits (eccentricities consistent with zero but with large errors $\sigma_e > 0.05$, dashed line). Both distributions are not corrected for the transit probability.

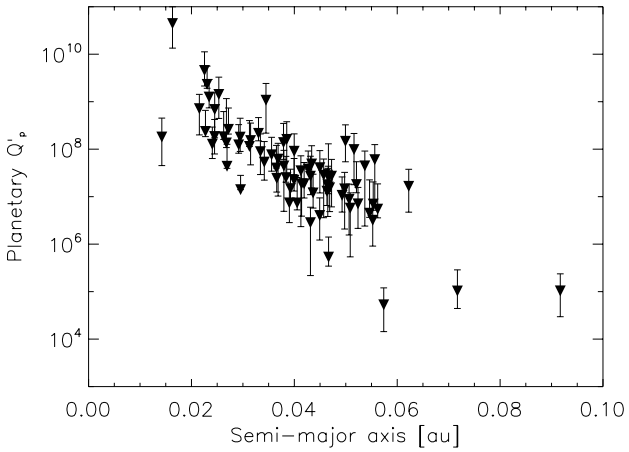

Figure 4: Upper limits of the planetary modified tidal quality factor $Q'_{\rm p}$ for clearly circular orbits ($\sigma_e < 0.05$) computed by using Eq. (7) in Matsumura et al. (2008). The large error bars are mainly due to the uncertainties on system ages.

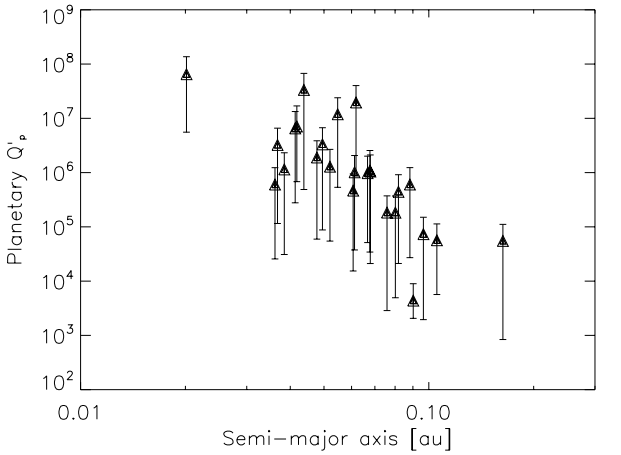

Figure 5: Lower limits of the planetary modified tidal quality factor $Q'_{\rm p}$ for eccentric orbits computed by using Eq. (8) in Matsumura et al. (2008). The large error bars are mainly due to the uncertainties on system ages.

Lower limits of $Q'_{\rm s}$ are displayed in Fig. 6 as a function of the planet orbital distance. The highest value $Q'_{\rm s} > 10^8$ is that of the star WASP-18 (whose hot Jupiter at $a = 0.02$ au has a small but significant eccentricity: $e = 0.0079 \pm 0.0010$), and is consistent with estimates relying on the timescales of the orbital decay of very hot Jupiters with $P \lesssim 1$ d (e.g., Ogilvie 2014). Fig. 7 shows an increase of $Q'_{\rm s}$ with stellar effective temperature thus suggesting that hotter stars undergo lower tidal dissipation because of their thinner convective zones, which is in agreement with the analytical results by Mathis (2015). This was invoked by Winn et al. (2010) to explain that misaligned hot-Jupiter systems are preferentially found around hotter stars, although alternative explanations have been considered, given the specific behaviour of tides in oblique systems (see, e.g., Lai 2012).

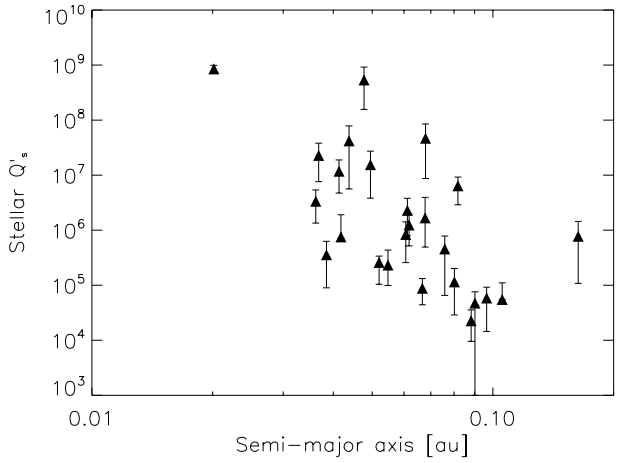

Figure 6: Lower limits of the modified tidal quality factor Q'_s of stars hosting eccentric planets computed by using Eq. (9) in Matsumura et al. (2008). The large error bars are mainly due to the uncertainties on system ages.

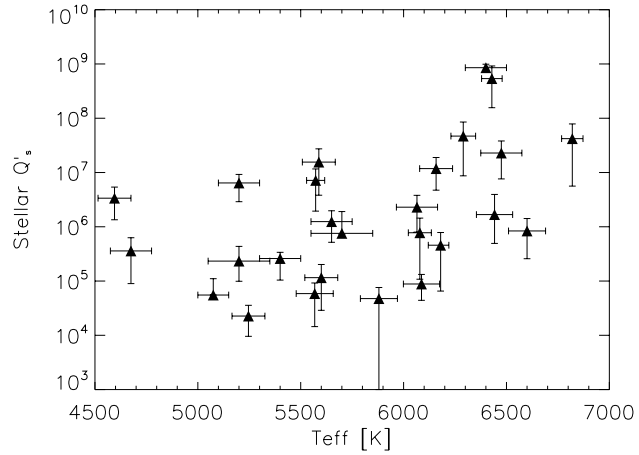

Figure 7: Lower limits of the modified tidal quality factor Q'_s of stars hosting eccentric planets as a function of stellar effective temperature.

5 Summary and conclusion

We carried out a Bayesian homogeneous determination of the orbital parameters of 211 TGP by analysing with our DE-MCMC tool both the literature RV data and new high-accuracy and high-precision RV measurements that were acquired with HARPS-N@TNG by the GAPS Consortium in the past three years. The goal of this analysis consists in determining accurate eccentricities and unveiling/characterizing long-term trends caused by outer stellar/planetary companions to understand better tidal star-planet interactions and the mechanisms responsible for the migration of close-in giant planets.

We found two new significant eccentricities, while four non-zero eccentricities that were previously reported in the literature turned out to be consistent with zero according to our analysis. We discovered the cold planetary companion of KELT-6b and revealed five long-term trends, two of which with the same slope as reported in the literature and the other three with different or inverted slope, which may indicate a curvature caused by an outer companion or an activity cycle (as for XO-2N). We did not detect any slope in two systems which were previously known to have such trends but this could be simply due to the fact that we sampled the maximum/minimum of the

curvature.

Our updated tidal diagram shows how tides raised on TGP by the host stars shape their orbital parameters, the most eccentric planets having high mass ratios and/or relatively large orbital separations, as expected from the equilibrium tidal theory. This would be the simple outcome of planetary migration from highly eccentric orbits that were originally produced by planet-planet scattering or Kozai-Lidov perturbations. Moreover, the $\alpha = a/a_R$ distribution peaking at $\gtrsim 2.7$ would also favour the aforementioned migration mechanism, if it is true that a clear imprint of the high-eccentricity migration is that the final orbital distance reached after circularisation must be greater or equal than twice the Roche limit from angular momentum conservation. The handful of TGP with $a < 2a_R$ may also be explained in the framework of high-eccentricity migration (Valsecchi & Rasio 2014).

This does not exclude that migration of close-in giant planets may occur via interactions with the protoplanetary disc. Two clear and recent examples of disc-migration are the planetary systems Kepler-101 (Bonomo et al. 2014) and WASP-47 (Becker et al. 2015). The first one is composed by an inner super-Neptune Kepler-101b with an orbital period $P = 3.49$ d and an outer Earth-size planet with $P = 6.03$ d. The latter contains four planets, with its hot Jupiter WASP-47b between an inner super-Earth ($P = 0.79$ d) and an outer Neptune-size planet ($P = 9.03$ d), and an additional long-period companion (Neveu-VanMalle et al. 2016). The TGP Kepler-101b and WASP-47b certainly migrated via disc interaction along with their close planetary companions otherwise the high-eccentricity migration would have caused gravitational interactions (with likely orbit crossings) and led to ejection and/or scattering of their low-mass companions. However, these systems seem to represent the exception rather than the rule because high-precision space-based data from Kepler and CoRoT revealed that the vast majority of hot giant planets do not have close companions (e.g., Latham et al. 2011). It is interesting to notice that warm Jupiters with orbital periods $10 < P < 200$ d have a much higher probability ($\sim 50\%$) of being found in compact multiple systems (Huang et al. 2016).

Approximately 33% (12%) of the eccentric (circular) TGP of our sample have an outer companion detected in the RV. This is in agreement with the results of a recent statistical study by Bryan et al. (2016) although the aforementioned rates do not take detection limits into account and thus are not corrected for survey incompleteness.

We provided upper and lower limits of the planetary modified tidal quality factors Q'_p and confirmed that high values of both Q'_p and Q'_s up to $10^8 - 10^9$ are required to explain the presence of the hottest giant planets on eccentric orbits. These high values of Q'_p are in agreement with the predicted very low internal dissipation in massive planets with a small core (Goodman & Lackner 2009).

Refined analyses with the addition of more recently discovered TGP will be the subject of a forthcoming paper.

References

Becker, J. C., Vanderburg, A., Adams, F. C., Rappaport, S. A., & Schwengeler, H. M. 2015, ApJL, 812, L18

Bonomo, A. S., Sozzetti, A., Lovis, C., et al. 2014, A&A, 572, A2

Bonomo, A. S., Sozzetti, A., Santerne, A., et al. 2015, A&A, 575, A85

Bryan, M. L., Knutson, H. A., Howard, A. W., et al. 2016, ArXiv e-prints

Cosentino, R., Lovis, C., Pepe, F., et al. 2012, in Society of Photo-Optical Instrumentation Engineers (SPIE) Conference Series, Vol. 8446, Society of Photo-Optical Instrumentation Engineers (SPIE) Conference Series, 1

Damasso, M., Biazzo, K., Bonomo, A. S., et al. 2015a, A&A, 575, A111

Damasso, M., Esposito, M., Nascimbeni, V., et al. 2015b, A&A, 581, L6

Damiani, C. & Lanza, A. F. 2015, A&A, 574, A39

Eastman, J., Gaudi, B. S., & Agol, E. 2013, PASP, 125, 83

Faber, J. A., Rasio, F. A., & Willems, B. 2005, Icarus, 175, 248

Fabrycky, D. & Tremaine, S. 2007, ApJ, 669, 1298

Ford, E. B. 2006, ApJ, 642, 505

Goldreich, P. & Tremaine, S. 1980, ApJ, 241, 425

Goodman, J. & Lackner, C. 2009, ApJ, 696, 2054

Huang, C. X., Wu, Y., & Triaud, A. H. M. J. 2016, ArXiv e-prints

Husnoo, N., Pont, F., Mazeh, T., et al. 2012, MNRAS, 422, 3151

Hut, P. 1981, A&A, 99, 126

Knutson, H. A., Fulton, B. J., Montet, B. T., et al. 2014, ApJ, 785, 126

Lai, D. 2012, MNRAS, 423, 486

Latham, D. W., Rowe, J. F., Quinn, S. N., et al. 2011, ApJL, 732, L24

Mandushev, G., O'Donovan, F. T., Charbonneau, D., et al. 2007, ApJL, 667, L195

Mathis, S. 2015, A&A, 580, L3

Matsumura, S., Takeda, G., & Rasio, F. A. 2008, ApJL, 686, L29

Murray, C. D. & Dermott, S. F. 1999, Solar system dynamics

Neveu-VanMalle, M., Queloz, D., Anderson, D. R., et al. 2016, A&A, 586, A93

Ogilvie, G. I. 2014, ARA&A, 52, 171

Papaloizou, J. C. B. & Larwood, J. D. 2000, MNRAS, 315, 823

Pont, F., Husnoo, N., Mazeh, T., & Fabrycky, D. 2011, MNRAS, 414, 1278

Rasio, F. A. & Ford, E. B. 1996, Science, 274, 954

Skillen, I., Pollacco, D., Collier Cameron, A., et al. 2009, A&A, 502, 391

Sozzetti, A., Bonomo, A. S., Biazzo, K., et al. 2015, A&A, 575, L15

Valsecchi, F. & Rasio, F. A. 2014, ApJL, 787, L9

Winn, J. N., Fabrycky, D., Albrecht, S., & Johnson, J. A. 2010, ApJL, 718, L145